CARBON letters

Original Articles
Carbon Letters Vol. 21, 8-15 (2017)

Thermoelectric Seebeck and Peltier effects of single walled carbon nanotube quantum dot nanodevice

H. A. El-Demsisy[1], M. D. Asham[1,♠], D. S. Louis[2] and A. H. Phillips[2]

[1]Faculty of Engineering, Benha University, Benha 13511, Egypt
[2]Faculty of Engineering, Ain-Shams University, Cairo 11535, Egypt

Article Info
Received 26 May 2016
Accepted 6 October 2016

♠Corresponding Author
E-mail: minadanial@yahoo.com
Tel: +20-01005080168

Open Access
DOI: http://dx.doi.org/10.5714/CL.2017.21.008

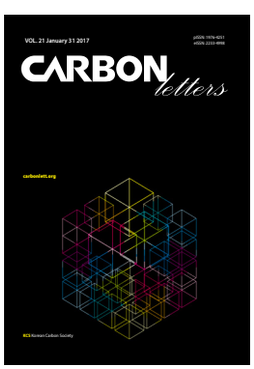

http://carbonlett.org

pISSN: 1976-4251
eISSN: 2233-4998

Abstract

The thermoelectric Seebeck and Peltier effects of a single walled carbon nanotube (SWCNT) quantum dot nanodevice are investigated, taking into consideration a certain value of applied tensile strain and induced ac-field with frequency in the terahertz (THz) range. This device is modeled as a SWCNT quantum dot connected to metallic leads. These two metallic leads operate as a source and a drain. In this three-terminal device, the conducting substance is the gate electrode. Another metallic gate is used to govern the electrostatics and the switching of the carbon nanotube channel. The substances at the carbon nanotube quantum dot/metal contact are controlled by the back gate. Results show that both the Seebeck and Peltier coefficients have random oscillation as a function of gate voltage in the Coulomb blockade regime for all types of SWCNT quantum dots. Also, the values of both the Seebeck and Peltier coefficients are enhanced, mainly due to the induced tensile strain. Results show that the three types of SWCNT quantum dot are good thermoelectric nanodevices for energy harvesting (Seebeck effect) and good coolers for nanoelectronic devices (Peltier effect).

Key words: armchair SWCNT, zigzag SWCNT, chiral SWCNT, Seebeck coefficient, Peltier coefficient

1. Introduction

The problem of waste heat recovery, e.g., from transportation vehicles and oil refineries, along with heat dissipation, e.g., in microelectronics, in which leakage currents in transistors exponentially increase with temperature, is of considerable relevance to the fields of energy generation and conservation. Thermoelectric materials can be used to convert heat to electricity through the Seebeck effect (say, in thermocouples), or can be used for cooling or refrigeration through the converse Peltier effect (say, for picnic coolers). Prevailing applications of thermoelectric devices are in the area of cooling, such as small and mobile refrigerators, temperature regulators of semiconductor lasers, and medical and scientific instruments; thermoelectric devices are also used for power generation [1]. Thermoelectric effects, including the Seebeck and Peltier effects, are the most straightforward methods of converting between thermal energy and electrical energy [2].

Recent achievements in the field of nanoscale systems have invigorated research activity in this area and renewed the quest for enhanced thermoelectric parameters, for example, Seebeck and Peltier coefficients [3]. Thermoelectric parameters are enhanced in structures with reduced dimensionality. In low dimensional systems, the density of states is reshaped with respect to bulk systems, in such a way that charge carriers are spread to higher energies [4]. This produces an increase not only of the Seebeck and Peltier coefficients but also, in principle, of the electrical conductivity and other thermoelectric parameters. Recently, the application of CNTs as a thermoelectric material has received interest for energy sensing, harvesting, and power generation [1,5]. The thermoelectric effect in single walled carbon

nanotubes (SWCNTs) is attractive because of the high thermo-power values measured in experiments [6,7]. It was found [8] that the thermo-power of SWCNTs could be modulated by the gate voltage. The unique electrical properties of carbon nanotubes continue to attract considerable interest because of this material's extraordinary nature and potential applications. Thermoelectric power, in particular, is sensitive to the balance of electrons and holes and electron mobility in a material, and therefore should be a valuable tool to elucidate the intrinsic electrical transport properties of SWCNTs [9,10]. The present authors [11,12] studied the quantum transport characteristics of a SWCNT quantum dot nanodevice under the effect of an external tensile strain. Armchair, zigzag, and chiral SWCNTs have been considered.

The purpose of the present paper is to investigate the thermoelectric Seebeck and Peltier effects of three types of SWCNT. Tuning the band gap of these three SWCNTs by tensile strain is taken into consideration.

2. The Model

A carbon nanotube field effect transistor (CNTFET) can be modeled as follows (Fig. 1): a SWCNT in the form of quantum dots is connected to two metallic leads. These two metallic leads operate as a source and a drain. In this three terminal device, the conducting substance is the gate electrode. Another metallic gate is used to govern the electrostatics and the switching of the carbon nanotube channel. The substances at the carbon nanotube quantum dot/ metal contact are controlled by the back gate.

The Dirac fermion electron tunneling through CNTFET is induced by an external applied ac-field, which is expressed as:

$$V=V_{ac}\cos\omega t \tag{1}$$

, where V_{ac} is the amplitude of the ac-field and ω is the field frequency. The thermo-power (Seebeck coefficient), S, and the Peltier coefficient (Π) are expressed in terms of the function L_m (μ), as follows [2,13,14]:

$$|S| = \frac{1}{eT}\cdot\frac{L_1}{L_0} \tag{2}$$

$$\Pi = \frac{L_1}{eL_0} \tag{3}$$

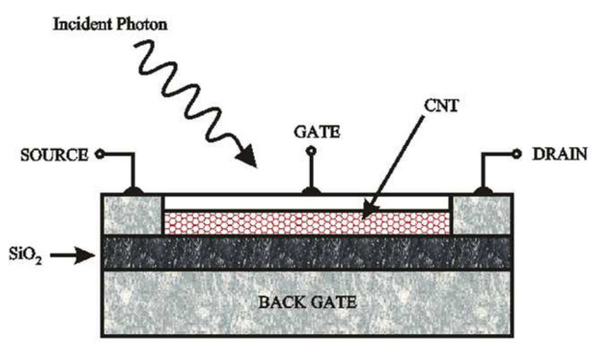

Fig. 1. Schematic diagram of the suggested model.

, where e is the electronic charge and T is the absolute temperature. The function, L_m, (for the cases m = 0, 1) is defined [1,2,13] in terms of the tunneling probability, $\Gamma_{with\ photons}(E)$, as follows:

$$L_m(\mu) = \frac{2}{h}\int_{E_F}^{E_F+\hbar\omega} dE\,\Gamma_{withPhoton}(E).(E-\mu)^m\cdot\left(-\frac{\partial f_{FD}(E)}{\partial E}\right) \tag{4}$$

, where h is Planck's constant, μ is the electrochemical potential, and $\left(-\partial f_{FD}(E)/\partial E\right)$ is the first derivative of the Fermi-Dirac distribution function and is given by:

$$\left(-\frac{\partial f_{FD}}{\partial E}\right) = \left(4k_BT\right)^{-1}.\cos h^{-2}\left(\frac{E-E_F+n\hbar\omega}{2k_BT}\right) \tag{5}$$

In which k_B is Boltzmann's constant, T is the absolute temperature, E is the energy of the tunneled electrons, E_F is the Fermi-energy, and $\hbar\omega$ is the photon energy of the induced ac-field. In eq 4, $\Gamma_{withphotons}(E)$ is the tunneling probability [11,12] expressed in terms of the tunneling probability without photons $\Gamma_{withoutphoton}(E-n'\hbar\omega)$ as follows [14-18]:

$$\Gamma_{withphoton}(E) = \sum_{n'=1}^{\infty} J_{n'}^2\left(\frac{eV_{ac}}{n'\hbar\omega}\right).f_{FD}\left(E-\left(\frac{C_{CNT}}{C}\right)eV_g-n'\hbar\omega-eV_{sd}\right).\Gamma_{withoutphoton}(E-n'\hbar\omega) \tag{6}$$

, where C_{CNT} is the capacitance of the SWCNT quantum dot, C is the coupling capacitance between the SWCNT quantum dot and the leads, V_g is the gate voltage, $\triangleq\omega$ is the energy of the induced photon, and J_n is the n'^{th} order Bessel function corresponding to the n'^{th} different side bands of the nanostructure carbon nanotube quantum dot. It was possible to determine the tunneling probability without the induction of the photons, $\Gamma_{withoutphoton}(E-n'\hbar\omega)$, using the WKB approximation method [18,19], as follows:

$$\Gamma_{withoutphoton}(E-n'\hbar\omega) = \exp\left[-2\int_{d}^{d+\Delta} dx\left(\frac{E_g}{\sqrt{3}a\gamma_0}\right).\sqrt{1-\left(\frac{E_1-n'\hbar\omega+eV_{sd}(1-x/L)}{\left(E_g/2\right)}\right)^2}\right] \tag{7}$$

, where a is the lattice constant, γ_o is the nearest neighbor hopping integral, E_g is the strained band gap energy, L is the length of the SWCNT quantum dot, d is the diameter of the SWCNT, and Δ is the SWCNT thickness. The energy (E_1) eq 7 is given by:

$$E_1 = E_F + eV_g + V_b + \frac{N^2e^2}{2C_{CNT}} + eV_{ac}\cos(\omega t) + \frac{\hbar eB}{2m^*} \tag{8}$$

, where E_F is the Fermi-energy, V_b is the barrier height at the interface between the SWCNT quantum dot and the leads, N is the number of tunneled electrons, e is the electronic charge, B is the applied magnetic field, and m^* is the effective mass of the charge carrier Dirac fermion. The strained band gap energy, E_g, is expressed in terms of the induced strain, ε, for each type of SWCNT, as follows [20]:

- For the armchair SWCNT, E_g is given by:

$$E_g = \left|\left(\frac{\gamma_0a^2}{16R^2}+\frac{ab\sqrt{3}}{2}\varepsilon\right).\sin(3\theta)\right| \tag{9}$$

-For the zigzag SWCNT, E_g is given by:

$$E_g = \left| \frac{\pi^2 \gamma_0}{4n^2} + \frac{ab\sqrt{3}}{2}\varepsilon \right| \quad (10)$$

- For the chiral SWCNT, E_g is given by:

$$E_g = \left| \left(\frac{\pi^2 \gamma_0}{8C_h^5} + \frac{ab\sqrt{3}}{4C_h^3}.\varepsilon \right).(n-m)(2n^2+5nm+m^2) \right| \quad (11)$$

, where b is the linear change in the transfer integral with a change in the bond length due to axial tensile strain, R is the radius of the carbon nanotube, θ is the chiral angle, and C_h is the chiral vector. The diameter (d) of the SWCNT, and the chiral angle (θ) are determined in terms of the chiral indices n and m [21-23] using the following equations:

$$d = \frac{a}{\pi}\left(n^2 + nm + m^2\right)^{\frac{1}{2}} \quad (12)$$

$$\cos(\theta) = \frac{2n+m}{2\sqrt{n^2+nm+m^2}} \quad (13)$$

The chiral vector (C_h) is expressed in terms of the chiral indices n and m as [21-23]:

$$C_h = \sqrt{n^2 + nm + m^2} \quad (14)$$

In the present paper we consider an armchair SWCNT, a zigzag SWCNT, and a chiral SWCNT; that is, for the armchair carbon nanotube $n = m$, while for zigzag carbon nanotube $m = 0$ [21-23], and for the chiral carbon nanotube with chiral indices n and m [24,25].

3. Results and Discussion

Numerical calculations are performed to determine the Seebeck coefficient, S, (eq 2) and the Peltier coefficient, Π, (eq 3) for the armchair SWCNT, the zigzag SWCNT, and the chiral SWCNT quantum dots nanodevices. The computations are performed for a specific value of strained energy gap (E_g) corresponding to the axial tensile strain (ε) which is approximately

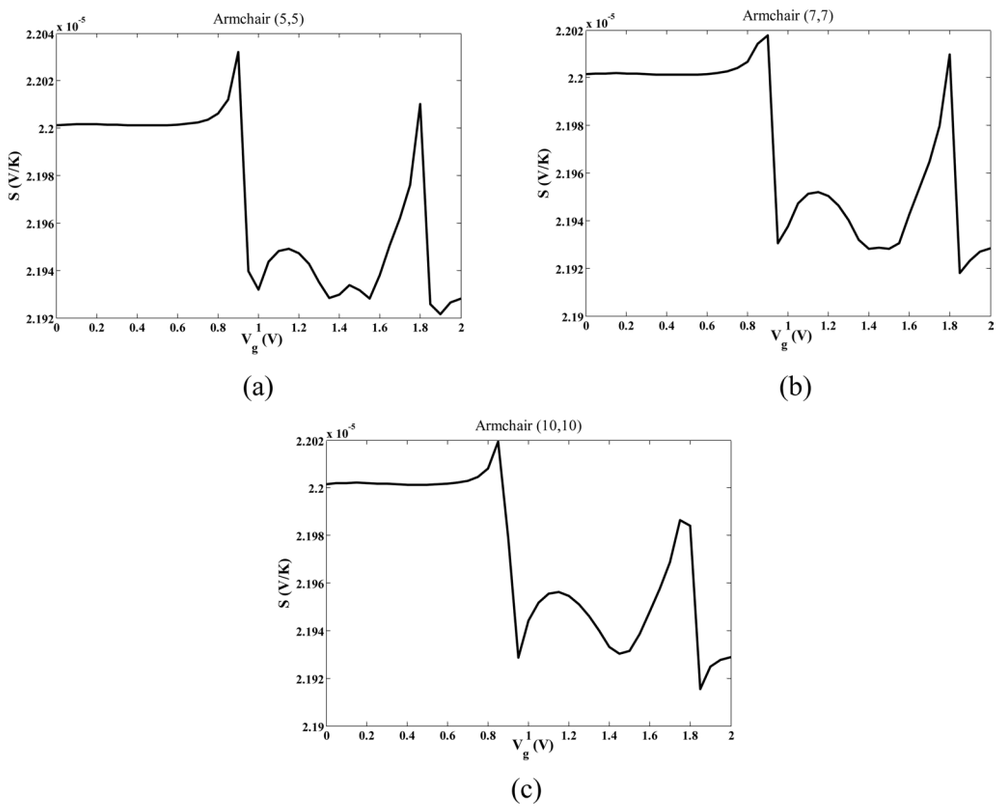

Fig. 2. Variation of the Seebeck coefficient (S) with the gate voltage (V_g) for armchair single walled carbon nanotube.

Table 1. Values of energy gaps of all single walled carbon nanotubes corresponding to ε = 0.1

	Armchair			Zigzag			Chiral		
	(5,5)	(7,7)	(10,10)	(6,0)	(7,0)	(9,0)	(6,2)	(6,3)	(8,3)
Energy gap (eV)		0.7456		0.9238	0.8766	0.8248	0.6304	0.546	0.4347

Axial tensile strain ε = 0.1.

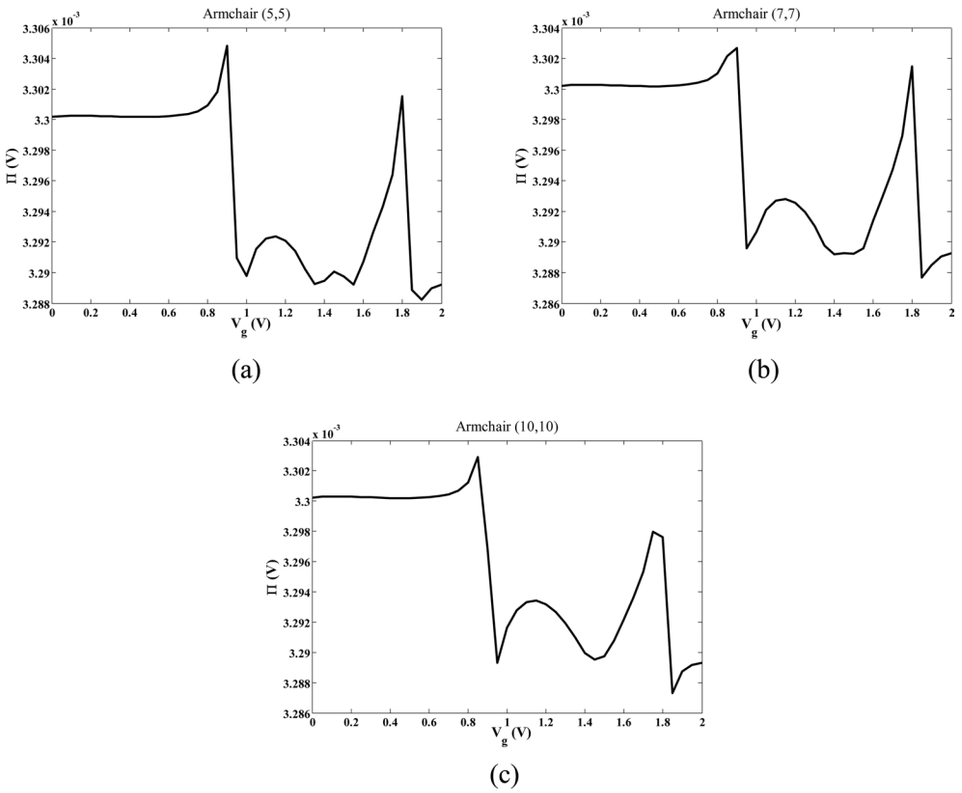

Fig. 3. Variation of Peltier coefficient (Π) with the gate voltage (V_g) for armchair single walled carbon nanotube.

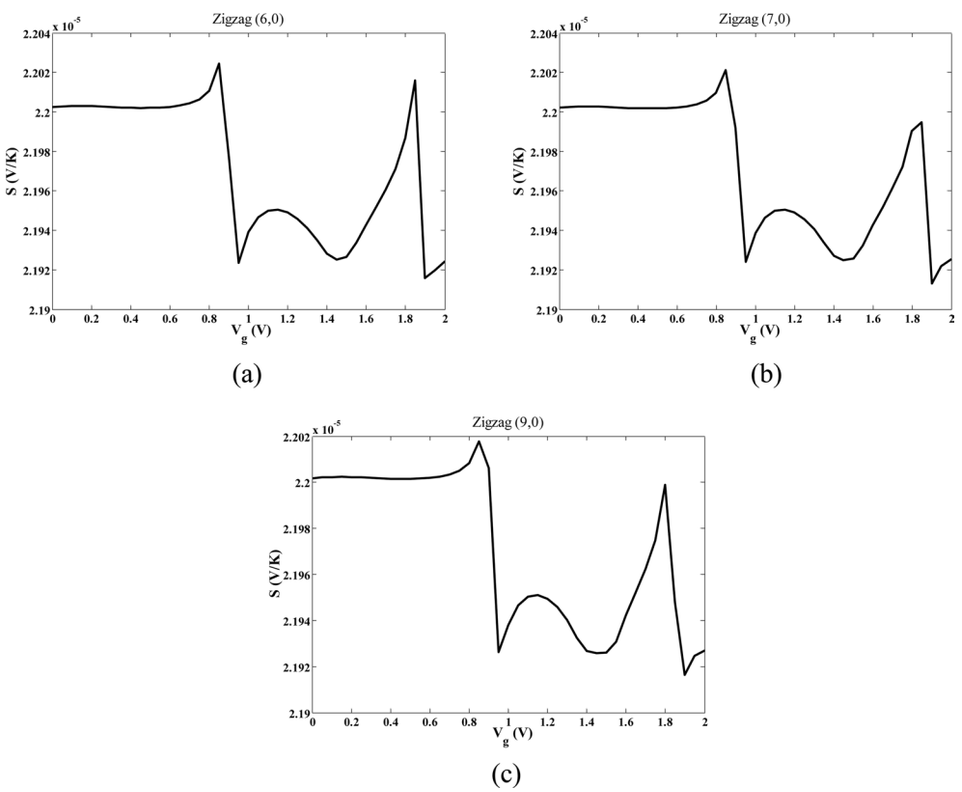

Fig. 4. Variation of the Seebeck coefficient (S) with the gate voltage (V_g) for zigzag single walled carbon nanotube.

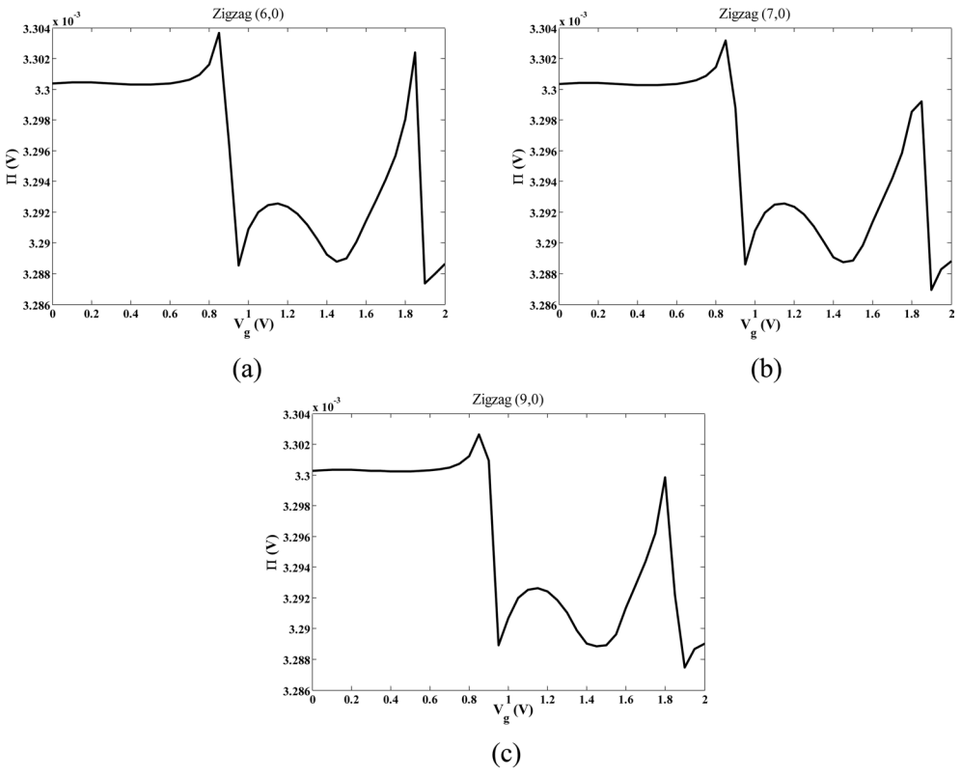

Fig. 5. Variation of Peltier coefficient (Π) with the gate voltage (V_g) for zigzag single walled carbon nanotube.

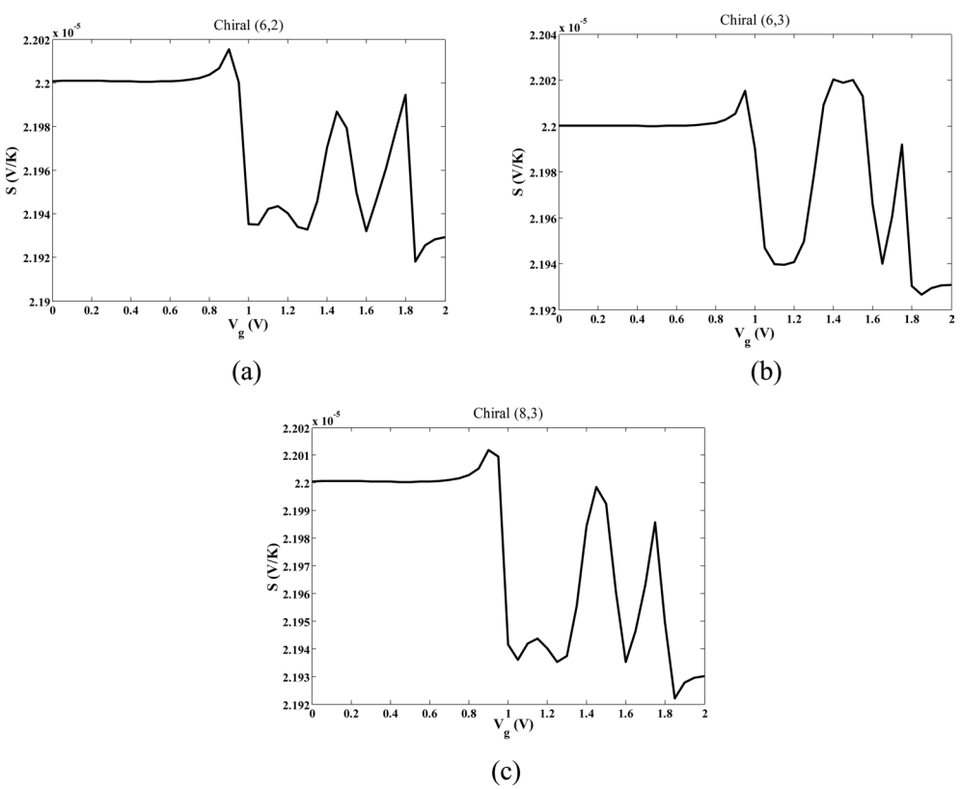

Fig. 6. Variation of the Seebeck coefficient (S) with the gate voltage (V_g) for chiral single walled carbon nanotube.

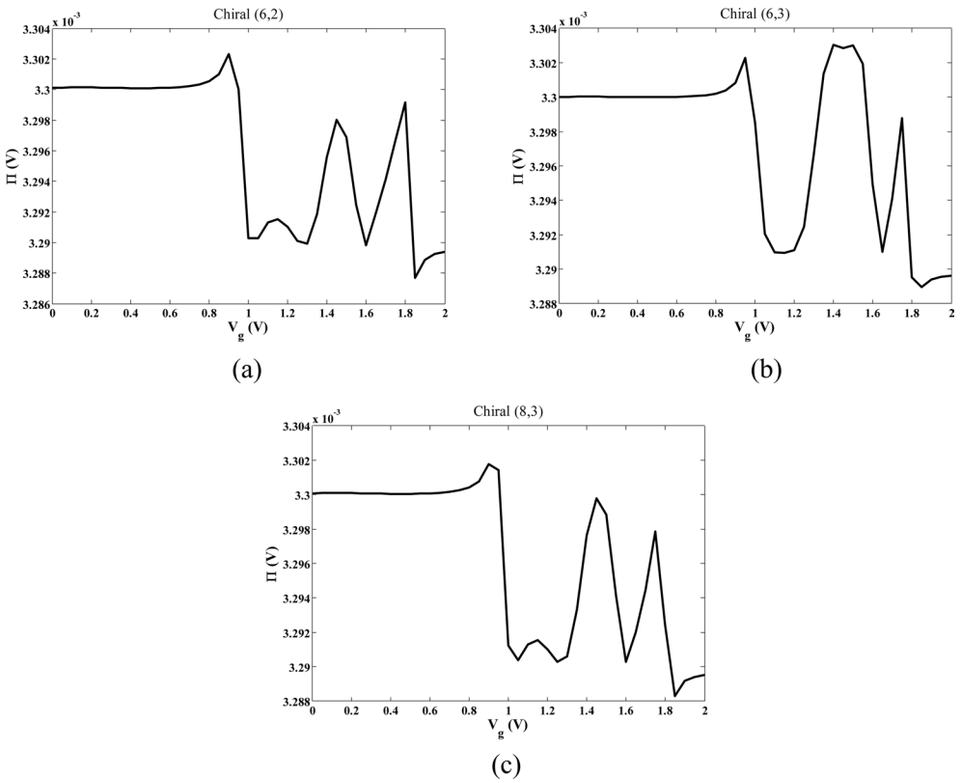

Fig. 7. Variation of Peltier coefficient (Π) with the gate voltage (V_g) for chiral single walled carbon nanotube.

equal to 0.1 (eqs 9-11) for all types of SWCNT and under an induced ac-field with a frequency in the mid-infrared range, that is, in the terahertz (THz) range. The Table 1 shows the values of the energy gaps for all types of SWCNT corresponding to a strain equal to 0.1. The features of the results are: Fig. 2 shows the variation of the Seebeck coefficient (S) with the gate voltage (V_g) for armchair SWCNTs of different chiral indices; Fig. 3 shows the variation of the Peltier coefficient (Π) with the gate voltage (V_g) for armchair SWCNTs of different chiral indices.

We notice in the Figs. 2 and 3 that the variations of both the Seebeck coefficient (S) and the Peltier coefficient (Π) oscillate with the dependence on the gate voltage (V_g) in a range of gate voltage from 0.9 V to 2.0 V. On the other hand, for small values of the gate voltage, that is, in the range 0 to approximately 0.84 V, we notice that there are slight variations of both the Seebeck coefficient and the Peltier coefficient. Fig. 4 shows the variation of Seebeck coefficient (S) with the gate voltage (V_g) for zigzag SWCNT of different values of chiral index (n) and Fig. 5 shows the variation of the Peltier coefficient (Π) with the gate voltage (V_g) for zigzag SWCNTs of different values of chiral index (n).

Oscillatory behavior of both the Seebeck coefficient (S) and the Peltier coefficient (Π) is observed with the dependence on the gate voltage (V_g) (Figs. 4 and 5). These oscillations of the investigated thermoelectric parameters S and Π start from approximately $V_g \cong 0.83$ V, and continue for higher values of the gate voltage. On the other hand, for small values of the gate voltage, that is, in the range 0 V to approximately 0.83 V, we notice that there are slight variations of both the Seebeck coefficient and the Peltier coefficient. Fig. 6 shows the variation of Seebeck coefficient (S) with the gate voltage (V_g) for chiral SWCNTs of different chiral indices, n and m. Fig. 7 shows the variation of the Peltier coefficient (Π) with the gate voltage (V_g) for chiral SWCNTs of different chiral indices, n and m.

Oscillatory behavior of both the Seebeck coefficient (S) and the Peltier coefficient (Π) is observed with the dependence on the gate voltage (V_g) (Figs. 6 and 7). These oscillations of the investigated thermoelectric parameters S and Π start from approximately $V_g \cong 0.85$ V and continue to higher values of the gate voltage. On the other hand, for small values of the gate voltage, that is, in the range 0 V to approximately 0.85 V, we notice that there are slight variations of both the Seebeck coefficient and the Peltier coefficient.

The present results for both the Seebeck and the Peltier coefficients show that the induced far-infrared radiation introduces new photon-mediated conduction channels in the devices [16,17,26,27]. The induced ac-field enhances the energy gap, and the density of states exhibits photon absorption and emission. The random oscillatory behavior of both the Seebeck and the Peltier coefficients results from the quantum nature of the SWCNTs with different chiral indices (armchair, zigzag, and chiral SWCNTs). Also, as shown in the Figs. 2-7 the general trend of the variation of both the Seebeck and Peltier coefficients with the gate voltage for all armchair, zigzag, and chiral SWCNTs is approximately the same. So, this trend can be explained as follows: The Seebeck coefficient and the Peltier coefficient of the three pairs from a range 0 to 0.7 V of the gate voltage are

constant, meaning that the resistance of the present investigated SWCNT quantum dot nanodevice is zero, and that the transistor as a result operates in the saturation mode [28-31]. In this regime, the bands are essentially straight, so that there is little scattering of electrons at the Fermi level. Then, from 0.7 to 0.9 V the Seebeck coefficient and the Peltier coefficient of the three pairs increase corresponding to the on state of the nanodevice. As the gate voltage is increased, both the Seebeck coefficient and the Peltier coefficient decrease sharply and the nanodevice enters the off regime. This regime is characterized by a large barrier in the middle of the SWCNT quantum dot that blocks the electrons (there is a small leakage current due to source–drain tunneling). As the gate voltage is further increased from 1.6 to 1.8 V, the channel is driven into inversion. In this case, the band bending creates an electrostatic quantum dot in the middle of the SWCNT, leading to the appearance of localized energy levels. Thus, the inversion regime in nanoscale SWCNT nanodevices consists of resonant tunneling through these discrete levels, leading to peaks in both the Seebeck coefficient and the Peltier coefficient [28-31]. These results are found to be concordant with those in literature [28-31]. Also, it can be observed that both the Seebeck and the Peltier coefficients have random oscillations as a function of the gate voltage in the Coulomb blockade regime for all types of SWCNT quantum dots [11,12,16,17,32-34]. In general, the values of both the Seebeck and the Peltier coefficients are enhanced mainly due to the induced axial tensile strain, such that the strain also has an important effect on the sub-band edges of the electron band structure by smoothing the steps in the electron transmission function (See eq 4) [10,35-37].

4. Conclusions

Numerical calculations are performed for the strained energy band gap for an armchair SWCNT, zigzag SWCNT, and chiral SWCNT. Also, for these materials, the diameter and the chiral angle are computed. Results show that for certain metallic SWCNTs with certain chiral indices there is a metallic SWCNT to semiconducting SWCNT transition. The variation of the energy band gap of all types of SWCNT with strain might be due to the breaking of the bond symmetry due to curvature of the three types of SWCNTs [11,12,36,37]. It is well known [21,24,25] that the in-plane C-C bond is a strong covalent σ bond, so the SWCNTs acquire a high elastic modulus along the axial direction. The authors [38-40] show that the maximum elastic tensile strain for SWCNTs is in the range 0.1–0.13 when studying mechanical properties of it. Therefore, in the present paper, we use a value of the axial tensile strain of 0.1. Accordingly, the values of the energy gap in the present investigated paper (Table 1) are in good agreement with those published for semiconducting SWCNT [11,12,22, 24,25].

The tuned band gap of all three types of SWCNT, due to external induced axial tensile strain, plays an important role in both the Seebeck and the Peltier coefficients. In the investigated armchair, zigzag, and chiral SWCNT quantum dots with band gap, electrons at the conduction sub-band edge make major contributions to the electron transport. From eq 4, it can be seen that these electrons have larger values of $(E - \mu)$, leading to larger values of L_1. As a result, both the Seebeck and the Peltier coefficients (eqs 2 and 3) are large, as predicted from the present results. This study can be important in studying flexible thermoelectric materials and thermal interface materials. The importance of both Seebeck and Peltier effects stems from the role of these effects in a variety of applications, from thermoelectric energy generation to technological applications such as spot cooling of integrated circuits and nanoelectronic devices. The results of the present research indicate that the quantum confined structure of SWCNT quantum dots (three types) may be promising for thermoelectric applications.

Conflict of Interest

No potential conflict of interest relevant to this article was reported.

References

[1] Goldsmid HJ. Introduction to Thermoelectricity, Springer-Verlag Berlin, Heidelberg (2010). https://doi.org/10.1007/978-3-642-00716-3.

[2] Wang JS, Wang J, Lü JT. Quantum thermal transport in nanostructures. Eur Phys J B, **62**, 381 (2008). https://doi.org/10.1140/epjb/e2008-00195-8.

[3] Dubi Y, Di Ventra M. Colloquium: heat flow and thermoelectricity in atomic and molecular junctions. Rev Mod Phys, **83**, 131 (2011). https://doi.org/10.1103/revmodphys.83.131.

[4] Minnich AJ, Dresselhaus MS, Ren ZF, Chen G. Bulk nanostructured thermoelectric materials: current research and future prospects. Energy Environ Sci, **2**, 466 (2009). https://doi.org/10.1039/B822664B.

[5] Jiang JW, Wang JS, Li B. A nonequilibrium Green's function study of thermoelectric properties in single-walled carbon nanotubes. J Appl Phys, **109**, 014326 (2011). https://doi.org/10.1063/1.3531573.

[6] Hone J, Ellwood I, Muno M, Mizel A, Cohen ML, Zettl A, Rinzler AG, Smalley RE. Thermoelectric power of single-walled carbon nanotubes. Phys Rev Lett, **80**, 1042 (1998). https://doi.org/10.1103/PhysRevLett.80.1042.

[7] Kong WJ, Lu L, Zhu HW, Wei BQ, Wu DH. Thermoelectric power of single-walled carbon nanotubes strand. J Phys Condens Matter, **17**, 1923 (2005). https://doi.org/10.1088/0953-8984/17/12/015.

[8] Small JP, Perez KM, Kim P. Modulation of thermoelectric power of individual carbon nanotubes. Phys Rev Lett, **91**, 256801 (2003). https://doi.org/10.1103/PhysRevLett.91.256801.

[9] Romero HE, Sumanasekera GU, Mahan GD, Eklund PC. Thermoelectric power of single-walled carbon nanotube films. Phys Rev B, **65**, 205410 (2002). https://doi.org/10.1103/PhysRevB.65.205410.

[10] Yao Q, Chen L, Zhang W, Liufu S, Chen X. Enhanced thermoelectric performance of single-walled carbon nanotubes/polyaniline hybrid nanocomposites. ACS Nano, **4**, 2445 (2010). https://doi.org/10.1021/nn1002562.

[11] El-Demsisy HA, Asham MD, Louis DS, Phillips AH. Coherent photo-electrical current manipulation of carbon nanotube field effect transistor induced by strain. Open Sci J Mod Phys, **2**, 27 (2015).

[12] El-Demsisy HA, Asham MD, Louis DS, Phillips AH. Strain effect on transport properties of chiral carbon nanotube nanodevice. Int J

Nanosci Nanoeng, **2**, 6 (2015).

[13] Esfarjani K, Zebarjadi M, Kawazoe Y. Thermoelectric properties of a nanocontact made of two-capped single-wall carbon nanotubes calculated within the tight-binding approximation. Phys Rev B, **73**, 085406 (2006). https://doi.org/10.1103/physrevb.73.085406.

[14] Bosnick K, Gabor N, McEuen P. Transport in carbon nanotube p-i-n diodes. Appl Phys Lett, **89**, 163121 (2006). https://doi.org/10.1063/1.2360895.

[15] Mina AN, Awadallah AA, Phillips AH, Ahmed RR. Microwave spectroscopy of carbon nanotube field effect transistor. Prog Phys, **4**, 61 (2010).

[16] Awadallah AA, Phillips AH, Mina AN, Ahmed RR. Photon-assisted transport in carbon nanotube mesoscopic device. Int J Nanosci, **10**, 419 (2011). https://doi.org/10.1142/S0219581X11008162.

[17] Platero G, Aguado R. Photon assisted transport in semiconductor nanostructures. Phys Rep, **395**, 1 (2004). https://doi.org/10.1016/j.physrep.2004.01.004.

[18] Nakanishi T, Bachtold A, Dekker C. Transport through the interface between a semiconducting carbon nanotube and a metal electrode. Phys Rev B, **66**, 073307 (2002). https://doi.org/10.1103/PhysRevB.66.073307.

[19] Heinze S, Radosavljević M, Tersoff J, Avouris P. Unexpected scaling of the performance of carbon nanotube Schottky-barrier transistors. Phys Rev B, **68**, 235418 (2003). https://doi.org/10.1103/PhysRevB.68.235418.

[20] Kleiner A, Eggert S. Band gaps of primary metallic carbon nanotubes. Phys Rev B, **63**, 073408 (2001). https://doi.org/10.1103/PhysRevB.63.073408.

[21] Satio R, Dresselhaus G, Dresselhaus MS. Physical Properties of Carbon Nanotubes, Imperial College Press, London (1998).

[22] Minot ED, Yaish Y, Sazonova V, Park JY, Brink M, Paul L, McEuen PL. Tuning carbon nanotube band gaps with strain. Phys Rev Lett, **90**, 156401 (2003). https://doi.org/10.1103/PhysRevLett.90.156401.

[23] Bhattacharya S, De D, Ghosh S, Ghatak KP. Fowler-Nordheim field emission from carbon nanotubes inder intense electric field. J Comput Theor Nanosci, **10**, 664 (2013). https://doi.org/10.1166/jctn.2013.2752.

[24] Mina AN, Awadallah AA, Phillips AH, Ahmed RR. Simulation of the band structure of graphene and carbon nanotube. J Phys Conf Ser, **343**, 012076 (2012). https://doi.org/10.1088/1742-6596/343/1/012076.

[25] Wong HSP, Akinwande D. Carbon Nanotube and Graphene Device Physics, Cambridge University Press, Cambridge (2011). https://doi.org/10.1017/CBO9780511778124.

[26] Zhao LN, Zhao HK. Coherent mesoscopic transport through a quantum dot-carbon nanotube system under two-photon irradiation. Eur Phys J B Condensed Matter Complex Syst, **42**, 285 (2004). https://doi.org/10.1140/epjb/e2004-00381-8.

[27] Pourfath M, Kosina H. Computational study of carbon-based electronics. J Comput Electron, **8**, 427, (2009). https://doi.org/10.1007/s10825-009-0285-z.

[28] Pimparkar N, Cao Q, Rogers JA, Alam MA. Theory and practice of "striping" for Improved ON/OFF ratio in carbon nanonet thin film transistors. Nano Res, **2**, 167 (2009). https://doi.org/10.1007/s12274-009-9013-z.

[29] Tan X, Liu H, Wen Y, Lv H, Pan L, Shi J, Tang X. Optimizing the thermoelectric performance of zigzag and chiral carbon nanotubes. Nanoscale Res Lett, **7**, 116 (2012). https://doi.org/10.1186/1556-276X-7-116.

[30] Guo J, Datta S, Lundstrom M. A numerical study of scaling issues for Schottky-barrier carbon nanotube transistors. IEEE Trans Electron Devices, **51**, 172 (2004). https://doi.org/10.1109/TED.2003.821883.

[31] Chen Z, Appenzeller J, Knoch J, Lin YM, Avouris P. The role of metal-nanotube contact in the performance of carbon nanotube field-effect transistors. Nano Lett, **5**, 1497 (2005). https://doi.org/10.1021/nl0508624.

[32] Mina AN, Zaki GH, Phillips AH. Coherent transport of carbon nanotube field effect transistor driven by AC-signal. Egypt J Phys, **42**, 21 (2011).

[33] Meyer C, Elzerman JM, Kouwenhoven LP. Photon-assisted tunneling in a carbon nanotube quantum dot. Nano Lett, **7**, 295 (2007). https://doi.org/10.1021/nl062273j.

[34] Awadalla AA, Phillips AH. Thermal shot noise through boundary roughness of carbon nanotube quantum dots. Chin Phys Lett, **28**, 017304 (2011). https://doi.org/10.1088/0256-307x/28/1/017304.

[35] Elseddawy AM, Zein WA, Phillips AH. Carbon nanotube-based nanoelectromechanical resonator as strain sensor. J Comput Theor Nanosci, **11**, 1174 (2014). https://doi.org/10.1166/jctn.2014.3478.

[36] Kanatzidis MG. Nanostructured thermoelectrics: the new paradigm? Chem Mater, **22**, 648 (2010). https://doi.org/10.1021/cm902195j.

[37] Ni ZH, Yu T, Lu YH, Wang YY, Feng YP, Shen ZX. Uniaxial strain on graphene: Raman spectroscopy study and band gap opening. ACS Nano, **2**, 2301 (2008). https://doi.org/10.1021/nn800459e.

[38] Yu MF, Files BS, Arepalli S, Ruoff RS. Tensile loading of ropes of single wall carbon nanotubes and their mechanical properties. Phys Rev Lett, **84**, 5552 (2000). https://doi.org/10.1103/PhysRevLett.84.5552.

[39] Tserpes KI, Papanikos P. The effect of Stone–Wales defect on the tensile behavior and fracture of single-walled carbon nanotubes. Compos Struct, **79**, 581 (2007). https://doi.org/10.1016/j.compstruct.2006.02.020.

[40] Zidour M, Hadji L, Bouazza M, Tounsi A, Bedia ElA. The mechanical properties of zigzag carbon nanotube using the energyyequivalent model. J Chem Mater Res, **3**, 9 (2015).